

# The Nature of Tunnel Splitting Mediated by Stacked Aromatics

Mikyung Lee,<sup>†</sup> Michael J. Shephard,<sup>‡</sup> Steven M. Risser,<sup>§</sup> Satyam Priyadarshy,<sup>†</sup>  
Michael N. Paddon-Row,<sup>‡,\*</sup> and David N. Beratan<sup>†,\*</sup>

Department of Chemistry, University of Pittsburgh, Pittsburgh, Pennsylvania 15260,  
School of Chemistry, University of New South Wales, Sydney 2052, Australia, and  
Core Technology Group, Battelle Memorial Institute, Columbus, Ohio 43201

Received: December 13, 1999; In Final Form: May 10, 2000

We have examined the distance and orientation dependence of the energy splitting,  $\Delta E(\pi^*)$ , between the two lowest-lying unoccupied molecular orbitals of a pair of tetracyanoethylene (TCNE) molecules bridged by a stack of noncovalently bonded benzene rings; the stack length ranged from one to six benzene molecules. The distance between ring planes was fixed at 3.4 Å, while the orientation of the rings and of the TCNE molecules was varied. The magnitude of the splitting energy was found to decay exponentially with increasing stack length,  $r$ ;  $\Delta E(\pi^*) = A \exp(-0.5\beta_e r)$ , with the damping factor,  $\beta_e$ , ranging in value from 1.1 to 1.6 Å<sup>-1</sup>, as might be anticipated for instances where the “tunneling energy” lies several electron volts away from the frontier orbitals of the  $\pi$ -electron stack. Both ab initio and semiempirical computations predict a weak dependence of the coupling upon the orientation of the rings. The ab initio HF/3-21G calculations give  $\beta_e$  values approximately 20% smaller than those values found in semiempirical computations using  $\pi$ -stacks in which the separation between adjacent benzene molecules (3.4 Å) is typical of stacked aromatic systems. This is due to the improved capability of the 3-21G basis set to treat the nearest-neighbor inter-ring orbital interactions, compared to the more contracted complete neglect of differential overlap (CNDO) basis set. Comparison to calculations with a more extended basis shows the 3-21G basis is accurate for rings separated by up to 4.0 Å, but for larger separations, ab initio calculations require the use of diffuse functions to properly describe the exponential decay of the interaction.

## 1. Introduction

The nature of electron tunneling interactions<sup>1–3</sup> across the noncovalent contacts of stacked aromatic systems, while of intense current interest in chemistry and biology, is rather poorly understood. Recently, considerable attention has turned to donor and acceptor groups at relatively fixed positions in DNA.<sup>4</sup> In stacked aromatics, the interplay between intramolecular and intermolecular effects on the tunneling propagation is not well understood from a theoretical perspective. Establishing a fundamental understanding of electron<sup>2,5</sup> and energy transfer<sup>6</sup> through aromatic stacks, including a description of competing mechanisms for single vs multistep<sup>1–3,5</sup> transport, will depend on establishing a molecular-level description of these tunneling interactions.

To illustrate the need for focused theoretical analysis of  $\pi$ -stacking tunneling processes, a wide range of experimentally determined distance dependencies have been reported for DNA electron transport.<sup>4</sup> The origin of this range of values is not presently understood. It is known that DNA electron transport can take place by a multistep hopping mechanism as well as by tunneling.<sup>1–5</sup> A current challenge to theory is to place quantitative bounds on the rate-controlling parameters in these varied mechanistic regimes, as well as to describe transitions between the regimes. The simple tunneling pathway analysis developed for proteins takes account of the qualitative difference

in the decay of through-bond and through-space wave function propagation.<sup>1</sup> However, in the case of large  $\pi$ -stacks, where the superexchange is dominated by through-space propagation between rings, simple pathway analysis—as formulated for proteins—is not applicable without substantial modification of parameters. The aim of this paper is to make a modest beginning with respect to the longer-term goals of the field of  $\pi$ -stack mediated tunneling. Specifically, we shall examine the dependence of the tunneling splitting between two tetracyanoethylene molecules (TCNE) placed at the ends of a stack comprising separate benzene rings, **1**( $n$ ) ( $n = 1–6$ , Scheme 1a).<sup>7</sup> These model systems were chosen: (1) to probe the distance and orientation dependence of  $\pi$ -stack mediated tunneling interactions in the regime of relatively large energy gaps between the donor/acceptor and the bridging states; (2) to compare the predictions of semiempirical and ab initio methods for stacked aromatic bridges; and (3) to examine the orientation dependence of tunneling interactions for highly symmetric (benzene) aromatic bridging units.

It is essential to note that the computations described here are not directly applicable to DNA electron transfer data, mainly because of (1) differences in the chemistries between a bridge consisting of benzene rings and a bridge consisting of base pairs with extended aromaticity and heteronuclear content; (2) differences in geometry between a benzene ring  $\pi$ -stack and a base pair helix; and (3) the wide range of donor/acceptor tunneling energetics probed in DNA experiments. Nonetheless, we hope that this study will provide the first comprehensive analysis of  $\pi$ -stack mediated tunneling interactions in the regime of high-symmetry bridges and large energy gaps between donor/acceptor

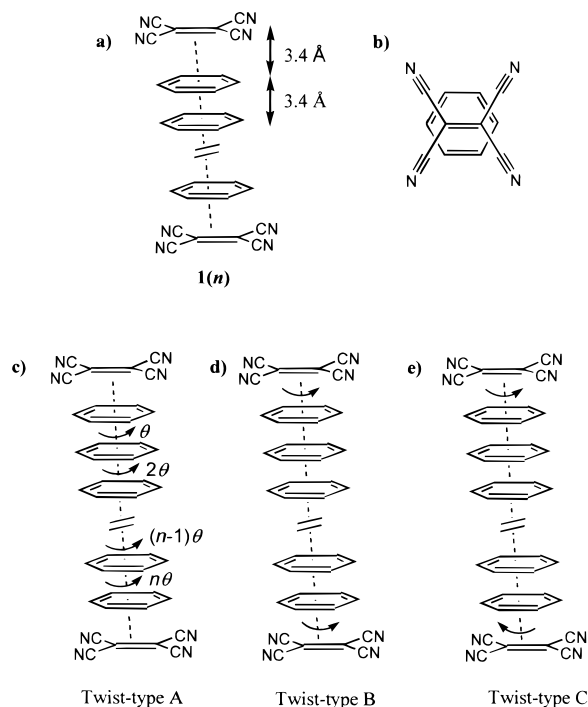
<sup>†</sup> University of Pittsburgh.

<sup>‡</sup> University of New South Wales.

<sup>§</sup> Battelle Memorial Institute.

\* To whom correspondence should be addressed.

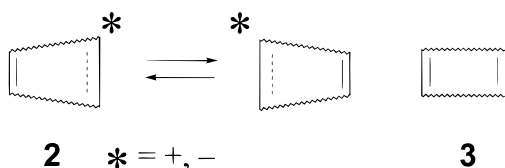
## SCHEME 1



and bridging states. In addition to establishing a benchmark for future studies of  $\pi$ -stack mediated coupling, this study should be of use in analyzing cyclophane-based electron transfer model systems which the University of New South Wales (UNSW) group is currently synthesizing (*vide infra*), and will provide a context for future analysis of  $\pi$ -stack mediated tunneling.

## 2. Computational Methods

The tunneling matrix element in a symmetric donor–acceptor system is one-half of the symmetric–antisymmetric splitting between the localized states. Jordan, Paddon-Row, and others have computed this splitting for fully covalent saturated hydrocarbon bridges using *ab initio* Hartree–Fock methods within the context of Koopmans’ theorem (KT).<sup>8–10</sup> For example, the KT-derived electronic coupling matrix element for intramolecular hole transfer (electron transfer) in a generic diene cation radical (anion radical), **2**, is equated to one-half of the  $\pi_{+, \pi^-}$  ( $\pi^*_{+, \pi^*_-}$ ) splitting energy calculated for the neutral ( $C_{2v}$ ) symmetric progenitor **3**.



Notwithstanding the shortcomings of the KT method, reliable predictions of electronic coupling interactions consistent with a rich experimental literature have emerged, and relatively simple “orbital symmetry rules” governing the tunneling propagation are now established.<sup>10</sup> Here, we expand this methodology and a related semiempirical method to electron tunneling in  $\pi$ -stacks.

The bridge geometries of **1(1)–1(6)** are a composite and were obtained by carrying out separate HF/3-21G level<sup>11</sup> geometry optimizations on a series of isolated stacks of benzene rings of overall  $D_{6h}$  symmetry, with the inter-ring separation frozen at

3.4 Å (all other degrees of freedom were optimized). The geometry for each of the two equivalent TCNE units was obtained from an HF/3-21G optimization of a single TCNE molecule constrained to  $D_{2h}$  symmetry. The complexes were then constructed by placing a TCNE molecule at each end of the  $\pi$ -stack in a plane parallel to, and 3.4 Å from the terminal benzene ring (see Scheme 1a). In addition to the fully eclipsed configuration ( $D_{2h}$  symmetry), illustrated by Scheme 1b, a number of other configurations of the **1(*n*)** complexes were examined by the application of different types and degrees of rotation, or “twist”, where the bridge and/or TCNE units were rotated around the axis passing through the centers of the two TCNE units.<sup>12</sup> Three rotational modes were examined. For twist-type A (Scheme 1c), upon descending the stack, each benzene ring is rotated by a fixed angle,  $\theta$ , with respect to its preceding neighbor; this results in a helical stack structure. The two TCNE molecules eclipse each other. For twist-type B (Scheme 1d), the two TCNE molecules are rotated in the same direction, and for twist-type C (Scheme 1e), the two TCNE molecules are rotated in opposite directions. In types B and C, the benzene rings remain unchanged in orientation.<sup>13</sup> These complexes were then used for either HF/3-21G level single-point energy calculations or complete neglect of differential overlap (CNDO) single-point calculations.

**Ab Initio Computation of Energy Splittings.** All *ab initio* calculations were carried out using the Gaussian 94 program.<sup>14</sup> Pairs of  $\pi^*_{+, \pi^*_-}$  splitting energies,  $\Delta E(\pi^*)$ , associated with the TCNE lowest unoccupied molecular orbitals (LUMOs) were then fitted to the exponential equation:

$$\Delta E(\pi^*) = A \exp(-0.5\beta_e r) \quad (1)$$

where  $\beta_e$  is a damping factor for the (hypothetical) electron-transfer process between the two TCNE chromophores in the anion radical, and  $r$  is the separation, in Å, between the two TCNE molecules.

**Semiempirical Computation of Energy Splittings.** The low computational cost and qualitative agreement with electron transfer experiments found using semiempirical methods makes them particularly appealing for studies of large electron-transfer systems. Indeed, recent applications of CNDO methods to protein and DNA electron transfer are plentiful.<sup>1,2,15</sup> The semiempirical CNDO calculations differ from the *ab initio* calculations in that a minimal, Slater-like, atomic orbital basis is used to describe only the valence electrons of the system. In addition, the Hamiltonian matrix elements that describe the energetics of the system are either determined from experimental data, or are only approximately determined in the CNDO calculations.

The reliability of semiempirical estimates of tunneling interactions seems to be somewhat system-dependent.<sup>16</sup> In this paper, we wish to explore the differences between *ab initio* and semiempirical methods in noncovalent  $\pi$ -stack structures. We will also examine the differences between calculation of the electronic interactions through orbital energy splittings, and a fragment-based approach. Calculations of the orbital energy splittings were performed using CNDO methods on the same geometries that were used in the *ab initio* calculation.

The calculations described above are based upon the determination of orbital-energy splittings in a self-consistent field (SCF) calculation; this is achieved by either direct diagonalization or by a Löwdin partitioning method.<sup>17</sup> As the splitting energy decreases in magnitude it becomes increasingly difficult to compute reliably. However, because the SCF computations do a good job of describing the relatively strong short-range

orbital interactions, even when the overall donor/acceptor splitting energy is poorly described, SCF results can remain useful in the regime of weak coupling. The fragment-based Löwdin energy splitting computation is carried out in stages. First, a computation is made of the interaction between the localized states (TCNE molecules) and the bridge. This is then combined with a computation of electronic propagation in the bridge itself. The expression for the coupling element in an orthogonal basis set (appropriate for the assumptions of the CNDO method) arises from Löwdin partitioning and may be written:<sup>17</sup>

$$\frac{\Delta E}{2} \approx \mathbf{C}_D \mathbf{V}_{DB} \mathbf{G}_B \mathbf{V}_{BA} \mathbf{C}_A \quad (2)$$

where the  $\mathbf{C}$  values represent the states localized on a single isolated TCNE,  $\mathbf{V}$  values represent the coupling between the TCNE and the bridge (the off-diagonal elements between TCNE and bridge orbitals in a full composite system calculation), and  $\mathbf{G}$  represents the bridging orbital Green functions (computed for the bridge in the absence of the TCNEs).  $\mathbf{G}$  for the bridge can be computed in two ways. One strategy to compute  $\mathbf{G}$  is to invert  $(E_t \mathbf{I} - \mathbf{F})$ , where  $\mathbf{F}$  is the Fock matrix for the bridge.  $E_t$  is chosen to be the energy eigenvalue associated with the TCNE localized LUMO in the calculation of the mixed TCNE-bridge system, consistent with the two-level system (Löwdin) reduction.<sup>17</sup> Another strategy is to compute the molecular orbitals of the isolated bridge and to calculate the matrix elements of the Green function operator via

$$\hat{G}(E_t) = \sum_{n(\text{occ})} \frac{|\varphi_n\rangle\langle\varphi_n|}{E_t - E_n} + \sum_{n'(\text{unocc})} \frac{|\varphi_{n'}\rangle\langle\varphi_{n'}|}{E_t - E_{n'}} \quad (3)$$

The reported energy splittings were computed at tunneling energies ( $E_t$ ) equal to the energy of the TCNE LUMO found for the isolated TCNE molecule.

### 3. Results

Within the context of simple McConnell theory, the overall electronic coupling between donor (D) and acceptor (A) in a D-bridge-A system may be represented as a product of two factors. One factor is due to coupling between the D (A) and the bridge, while the other is due to propagation of the coupling through the bridge, resulting from interactions among the bridge units (intra-bridge coupling).<sup>10b,18</sup> The latter factor involves contributions arising from all possible intra-bridge coupling pathways, two examples of which are illustrated in Figure 1. Pathway (a) involves only interactions between nearest-neighbor benzene groups, whereas pathway (b), in addition to the nearest-neighbor interactions, also includes an interaction involving more remote bridge units (a non-nearest-neighbor interaction). Because the intra-bridge coupling has a significant influence on both the magnitude and distance dependence of the net splitting between the two chromophores,<sup>10,19</sup> it is necessary to examine this aspect in some detail. In particular, it is useful to determine if the nearest-neighbor coupling pathway (Figure 1a) is the dominant contributor to the intra-bridge coupling or whether any pathways involving non-nearest-neighbor couplings (e.g., Figure 1b) also need to be taken into account. This question may be conveniently answered in the case of the  $\pi$ -stack bridge of  $\mathbf{1}(n)$  by calculating the strength of the coupling between two benzene rings for various inter-benzene separations corresponding to the various interactions that might be present in the  $\pi$ -stack, e.g., 3.4 Å separation corresponds to the nearest-

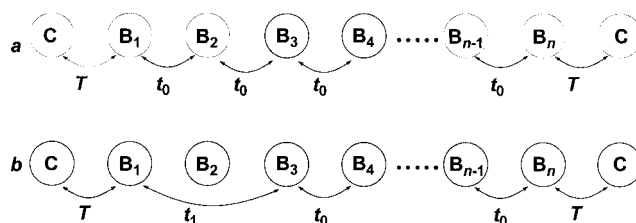


**Figure 1.** Two examples of coupling pathways for a system comprising two chromophores, C, and a chain of  $n$  bridge subunits,  $B_i$  (e.g., benzene rings in the present context). In this scheme, the strength of the coupling between the chromophores and the bridge is denoted by  $T$  and that between bridge subunits is denoted by  $t_0$  for nearest-neighbor interactions,  $t_1$  for next-nearest-neighbor interactions, etc. (a) This coupling pathway comprised exclusively nearest-neighbor interactions through the bridge. Within the context of the McConnell model,<sup>10b,18</sup> the contribution of this pathway to the splitting energy is given by  $\Delta E_a = -2(T^2/\Delta)(t_0/\Delta)^{n-1}$ , where  $\Delta$  is the energy gap between the chromophore and the bridge states (assuming that the bridge is composed of identical units and that the chromophores are the same). (b) A coupling pathway involving a single non-nearest-neighbor interaction, all other interactions being of the nearest-neighbor kind. The (McConnell) contribution of this pathway to the overall splitting is given by  $\Delta E_b = -2(T^2/\Delta)(t_0/\Delta)^{n-3}(t_1/\Delta)$ . The total splitting energy,  $\Delta E$ , between the chromophores is given by the sum of contributions from all possible pathways, including those that retrace pathways  $\Delta E = \Delta E_a + \Delta E_b \dots$ <sup>10b</sup>

neighbor interaction, 6.8 Å separation corresponds to the next-nearest-neighbor interaction, and so on.

In this spirit, the through-space coupling between the  $e_{1g}$  highest occupied molecular orbitals (HOMOs) of two benzene rings was examined as a function of their separation. KT-based, HF/3-21G calculations on an isolated benzene dimer possessing  $D_{6h}$  symmetry give a large through-space  $\pi$ -splitting energy,  $\Delta E(\pi)$ , of 1.15 eV at 3.4 Å separation, but which decays rapidly to give a value of 0.2 meV at 6.8 Å separation. Calculations with the HF/6-31+G give a splitting energy at 3.4 Å separation, 1.19 eV, which is nearly the same as the HF/3-21G value at the same separation (1.15 eV). However, the calculated splitting at 6.8 Å separation (8 meV) is 40 times larger than the HF/3-21G value. These results are similar to those obtained earlier for the through-space coupling between two ethene molecules.<sup>10a</sup> Further calculations using the even more flexible 6-311+G(d) basis set gave essentially the same splitting energies at 3.4 and 6.8 Å separations as those obtained using the 6-31+G basis set.

We have determined a distance decay factor for the splitting from a series of KT-based calculations where the separation between the rings was increased in increments of 0.1 Å. The distance dependence of the HF/3-21G splitting energy displays marked nonexponential behavior, with  $\beta_h$  substantially increasing from 2.89 to 7.88 Å<sup>-1</sup>, upon increasing the benzene-benzene separation from 3.4 to 6.8 Å.<sup>20</sup> The calculated  $\Delta E(\pi)$  values for the benzene dimer using the more diffuse 6-31+G basis set exhibited reasonable exponential behavior, with  $\beta_h$  increasing slightly, from 2.75 to 2.99 Å<sup>-1</sup>, over the 3.4–6.8 Å range of benzene-benzene separations. Similar calculations using the CNDO methods give a larger distance dependence,  $\beta_h = 3.89$  Å<sup>-1</sup> at 3.4 Å, that is approximately 30% larger than the ab initio values. However, the CNDO  $\beta_h$  value increases only modestly, reaching a value of 5.09 Å<sup>-1</sup> at 6.8 Å. Note that these values of  $\beta_h$  are large, because they measure the distance decay of the splitting due to tunneling through vacuum between the rings.

The HF/6-31+G data for the benzene dimer lead to the important conclusion that the coupling between two benzene rings 6.8 Å apart, or greater, is 2 orders of magnitude weaker

**TABLE 1: KT HF/3-21G  $\Delta E(\pi^*)$  Splitting Energies (eV) Obtained from the Application of Twist-Type A to  $1(n)$** 

$(n)$	$\Delta E(\pi^*)$ (eV) for specified twist angles					
	$0^\circ$	$6^\circ$	$12^\circ$	$18^\circ$	$24^\circ$	$30^\circ$
1	0.1061	0.1062	0.1065	0.1070	0.1073	0.1075
2	0.01695	0.01695	0.01695	0.01695	0.01693	0.01691
3	0.00245	0.00245	0.00244	0.00242	0.00241	0.00241
4	$3.32 \times 10^{-4}$	$3.31 \times 10^{-4}$	$3.28 \times 10^{-4}$	$3.25 \times 10^{-4}$	$3.25 \times 10^{-4}$	$3.28 \times 10^{-4}$
5	$4.31 \times 10^{-5}$	$4.28 \times 10^{-5}$	$4.22 \times 10^{-5}$	$4.21 \times 10^{-5}$	$4.25 \times 10^{-5}$	$4.28 \times 10^{-5}$
6	$5.43 \times 10^{-6}$	$5.36 \times 10^{-6}$	$5.29 \times 10^{-6}$	$5.34 \times 10^{-6}$	$5.37 \times 10^{-6}$	$5.32 \times 10^{-6}$

than that between benzene rings 3.4 Å apart. Consequently, to a very good approximation, the superexchange coupling through a stack of benzene rings with nearest-neighbor separations of 3.4 Å is largely determined by the pathway depicted in Figure 1a, involving only nearest-neighbor interactions, and that pathways involving longer range coupling, such as that depicted in Figure 1b, may be ignored. The good agreement between the HF/3-21G and the HF/6-31+G  $\Delta E(\pi)$  values for the benzene dimer at 3.4 Å separation also suggests that the less expensive 3-21G basis set is adequate for investigating electronic coupling in  $1(n)$  and this procedure will be adopted here. Furthermore, the dominance of nearest-neighbor interactions in the  $\pi$ -stack of  $1(n)$  should allow qualitative analysis of the coupling in this system to be made using a nearest-neighbor model, although the adequacy of this low-order nearest-neighbor perturbation-theory treatment (McConnell-like models<sup>18</sup>) of the splitting will depend on the value of the tunneling energy.

However, both the nonexponential decay of  $\Delta E(\pi)$  and the very small value for the splitting at 6.8 Å separation also set restrictions on the validity of this approach. The compact nature of the 3-21G basis limits its applicability to systems where the interorbital separations are within approximately 4 Å.<sup>8b</sup> In this model system, where the closest second-nearest neighbor sites are 6.8 Å distant, and thus only very weakly interact, we are justified in neglecting these interactions and using a compact basis. In more complex systems, such as proteins, where the interorbital separations have a more continuous range, the 3-21G basis may not be sufficient. However, this problem can be overcome by using more flexible basis sets.

The magnitude and distance dependence characteristics of the HF/3-21G  $\pi^*$  splitting energy,  $\Delta E(\pi^*)$ , resulting from the interaction between the  $e_{2g}$  LUMOs of the benzene molecules in the dimer, are similar to those for the  $\Delta E(\pi)$  values. Thus,  $\Delta E(\pi^*)$  decreases from 1.21 eV at 3.4 Å separation, to 0.2 meV at 6.8 Å separation, and it displays marked nonexponential distance dependence behavior, the damping factor,  $\beta_e$ , increasing from 2.56 to 7.90 Å<sup>-1</sup>, with increasing inter-benzene separation, from 3.4 to 6.8 Å. Values for  $\pi^*$  coupling at the HF/6-31+G level were not determined owing to the presence of discretized continuum functions in the virtual manifold using this basis set.<sup>21</sup>

Another important factor in the distance decay dependence of electron transfer in a donor-bridge-acceptor system such as  $1(n)$  is the magnitude of the energy gap,  $\Delta$ , between the relevant frontier MOs of the donor/acceptor chromophores and the frontier MOs of the bridge. Previous calculations have shown that  $\Delta$  can have a profound influence on both the rate of decay and the degree of deviation from exponential behavior of the coupling.<sup>10c,10d,19,22</sup> However, HF/3-21G calculations on the isolated  $\pi$ -stacks of  $1(n)$  (i.e., in the absence of the two TCNE molecules) reveal, with the exception of the first two members of the series, that the frontier MO energy levels of the  $\pi$ -stack change only modestly with increasing  $\pi$ -stack length, with the HOMO energy increasing gradually from -7.96 eV, in the case of the three-benzene stack, to -7.51 eV, in the case of the six-benzene stack, while the LUMO energy decreases only slightly,

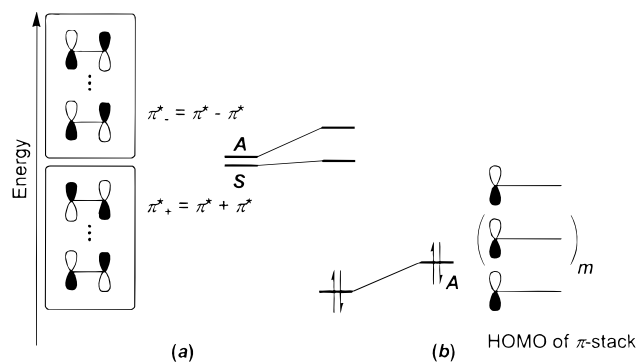


**Figure 2.** Frontier orbital description of the level sequence of the TCNE LUMOs. (a) Symmetry-adapted through-space mixing of the TCNE LUMOs producing the normal sequence of levels, i.e.,  $\pi^*_-$  below  $\pi^*_+$ . (b) Schematic of part of the HOMO of the  $\pi$ -stack illustrating the nodal structure (horizontal lines are the benzene rings). Symmetry labels  $A$  and  $S$  refer to plane of symmetry which is perpendicular to, and bisects the  $C_6$  symmetry axis passing through the  $\pi$ -stack of  $1(n)$ .

from 3.72 to 3.70 eV.<sup>23</sup> Similar changes are observed with the HF/6-31+G and CNDO results. Calculations on isolated TCNE molecules give LUMO energy of approximately -0.9 eV. Therefore, variation in  $\Delta$  as the bridge is lengthened should not play a significant role in determining the distance decay dependence of the TCNE  $\pi^*$ ,  $\pi^*$  splitting energies in  $1(n)$ .

We turn now to  $\pi^*$ ,  $\pi^*$  interactions ( $\Delta E(\pi^*)$ ,  $\beta_e$ ) involving the TCNE LUMOs in the TCNE-capped  $\pi$ -stacks  $1(n)$ . The HF/3-21G  $\Delta E(\pi^*)$  splitting energies for the fully eclipsed ( $D_{2h}$  symmetry) configuration of  $1(n)$  show a rapid decay with increasing bridge length, decreasing by 5 orders of magnitude from  $1(1)$  to  $1(6)$  (Table 1,  $0^\circ$  twist values). The  $\beta_e$  values reveal a slight deviation from exponential behavior, increasing from 1.08 Å<sup>-1</sup> ( $\beta_e(1,2)$ ) to a limiting value of 1.22 Å<sup>-1</sup> ( $\beta_e(5,6)$ ). The calculations show that the two TCNE  $\pi^*$  LUMOs for all members of the series  $1(n)$  studied follow the “normal” sequence rather than the “inverted” sequence;<sup>24</sup> that is, the symmetric ( $S$ ) combination of TCNE LUMOs,  $\pi^*_+ = \pi^* + \pi^*$ , lies energetically below the antisymmetric ( $A$ ) combination,  $\pi^*_- = \pi^* - \pi^*$ , rather than the reverse (Figure 2a). This invariance of the level sequence to the parity of the number of benzene rings in the  $\pi$ -stack has a simple frontier molecular orbital (MO) explanation. The HOMO of the isolated  $\pi$ -stack may be regarded as being formed from that combination of HOMOs of the component benzene rings which gives the maximum number of nodes (Figure 2b). This MO must therefore be antisymmetric with respect to the symmetry plane perpendicular to and bisecting the  $C_6$  symmetry axis passing through the  $\pi$ -stack. Consequently, mixing of the  $\pi$ -stack HOMO with the antisymmetric combination of TCNE LUMOs,  $\pi^*_-$ , will push  $\pi^*_-$  above  $\pi^*_+$ , thereby leading to the observed normal sequence of levels.<sup>24d</sup>

The HF/3-21G  $\Delta E(\pi^*)$  splitting energies obtained for  $1(n)$  are insensitive to the relative twisting orientations of the individual benzene molecules of the stack (twist-type A, Table 1),

**TABLE 2: Direct Diagonalization CNDO  $\Delta E(\pi^*)$  Splitting Energies (eV) Obtained from the Application of Twist-Type A to  $1(n)$** 

(n)	$\Delta E(\pi^*)$ (eV) for specified twist angles					
	0°	6°	12°	18°	24°	30°
1	0.03851	0.03851	0.03851	0.03851	0.03851	0.03851
2	0.00348	0.00348	0.00347	0.00345	0.00344	0.00344
3	$2.70 \times 10^{-4}$	$2.70 \times 10^{-4}$	$2.68 \times 10^{-4}$	$2.67 \times 10^{-4}$	$2.65 \times 10^{-4}$	$2.65 \times 10^{-4}$
4	$1.96 \times 10^{-5}$	$1.95 \times 10^{-5}$	$1.93 \times 10^{-5}$	$1.92 \times 10^{-5}$	$1.91 \times 10^{-5}$	$1.91 \times 10^{-5}$
5	$1.35 \times 10^{-6}$	$1.34 \times 10^{-6}$	$1.33 \times 10^{-6}$	$1.32 \times 10^{-6}$	$1.31 \times 10^{-6}$	$1.31 \times 10^{-6}$
6	$9.00 \times 10^{-8}$	$8.92 \times 10^{-8}$	$8.82 \times 10^{-8}$	$8.74 \times 10^{-8}$	$8.68 \times 10^{-8}$	$8.63 \times 10^{-8}$

**TABLE 3: Löwdin/CNDO Based Semiempirical  $\Delta E(\pi^*)$  Splitting Energies Divided by 2 (eV) Obtained from the Application of Twist-Type A to  $1(n)$** 

(n)	$\Delta E(\pi^*)$ (eV) for specified twist angles					
	0°	6°	12°	18°	24°	30°
1	0.02885	0.02882	0.02879	0.02879	0.02876	0.02875
2	0.00304	0.00296	0.00296	0.00295	0.00294	0.00294
3	$2.40 \times 10^{-4}$	$2.28 \times 10^{-4}$	$2.38 \times 10^{-4}$	$2.38 \times 10^{-4}$	$2.37 \times 10^{-4}$	$2.36 \times 10^{-4}$
4	$1.74 \times 10^{-5}$	$1.73 \times 10^{-5}$	$1.72 \times 10^{-5}$	$1.71 \times 10^{-5}$	$1.70 \times 10^{-5}$	$1.70 \times 10^{-5}$
5	$1.20 \times 10^{-6}$	$1.19 \times 10^{-6}$	$1.18 \times 10^{-6}$	$1.17 \times 10^{-6}$	$1.16 \times 10^{-6}$	$1.16 \times 10^{-6}$
6	$7.94 \times 10^{-8}$	$6.44 \times 10^{-8}$	$6.42 \times 10^{-8}$	$6.32 \times 10^{-8}$	$6.25 \times 10^{-8}$	$6.16 \times 10^{-8}$

**TABLE 4: Distance Decay Constants,  $\beta_e$ , (per Å)<sup>a</sup> Computed from Each Pair of Calculated  $\Delta E(\pi^*)$  Values**

(n)	$\beta_e(n,n+1)$		
	ab initio (±0.01)	CNDO (full diagonalization) (±0.01)	CNDO (Löwdin) (±0.03)
1	1.08	1.41	1.33
2	1.14	1.50	1.49
3	1.18	1.54	1.54
4	1.20	1.57	1.58
5	1.22	1.59	1.61

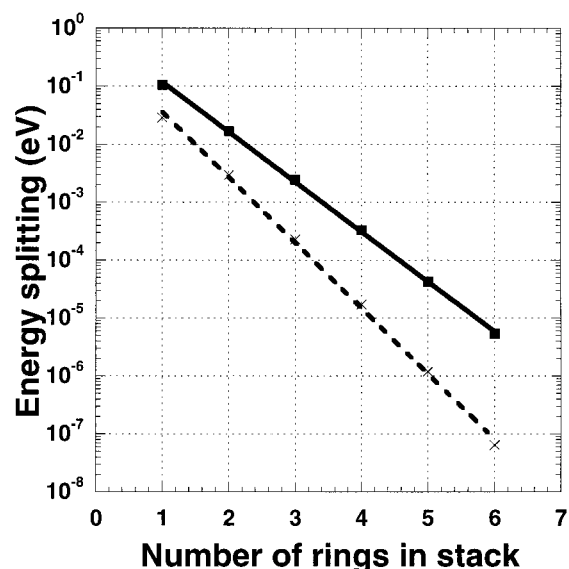
<sup>a</sup> Within the quoted uncertainties, the decay constants are independent of the twist-type.

with the magnitude of the coupling changing by less than 3% for any of the rotation angles.

Tables 2 and 3 present the CNDO splitting energies for  $1(n)$ , calculated directly, or through the perturbation expansion. The CNDO splitting energies are smaller than the ab initio values, by a factor of 3 for a single benzene ring, increasing to 2 orders of magnitude for a stack of 6 benzene rings. Despite this numerical difference at large distances between the methods, the  $\beta_e$  values (Table 4) differ by only 30%. The CNDO energy splittings (resulting from computations on the full TCNE–benzene–TCNE stacks) match very closely the values computed using the Löwdin partitioning approximation.

The rapid decay of the splitting with a number of intervening benzenes can be represented approximately by an exponential function, with the damping factor  $\beta_e$  determining the rapidity of the decrease. Table 4 gives the calculated  $\beta_e$  values for the splittings shown in Tables 1–3. These values were determined using the changes in the splitting as the number of benzene rings is increased. For all three sets of calculational methods, it is seen that  $\beta_e$  displays a small increase with increasing number of benzene molecules. The HF/3-21G  $\beta_e$  values are substantially smaller than the corresponding CNDO values, again reflecting the greater flexibility of the 3-21G basis set in treating the interaction between adjacent rings. Comparisons of the ab initio and semiempirical calculations are shown in Figure 3 for all three twist types and for a 6° angle.

The HF/3-21G  $\Delta E(\pi^*)$  splitting energies obtained for  $1(n)$  are insensitive to the orientation of the chromophores with respect to the bridge (twist-type B, Table 3). Regardless of the degree of twisting, the  $\Delta E(\pi^*)$  splitting energies and the  $\beta_e$

**Figure 3.** KT HF/3-21G (solid line) and semiempirical (dashed line)  $\pi^*$  splitting energies obtained from application of twist-types A, B, and C with a rotation angle of 6° for the  $1(n)$   $\pi$ -stack series.

values are very similar to those obtained for the fully eclipsed,  $D_{2h}$  configuration. For twist-type C (Table 6), the  $\Delta E(\pi^*)$  values decrease with increasing twisting angle, but this is due to the increasing degree of orthogonality between the TCNE molecules, as shown in Figure 4. The  $\beta_e$  values for twist-type C are still similar to those obtained for twist-types A and B (Tables 1 and 5), indicating that the  $\pi$ -stack still couples the two TCNE molecules, albeit with a reduced magnitude. The CNDO results are very similar in behavior, and are included in the Supporting Information.

#### 4. Conclusions

We have examined  $\pi$ -mediated electronic communication in the regime where the “donor and acceptor” states are several electron volts removed from the bridge states. We find that the exponential damping factor,  $\beta_e$ , governing the drop-off of splitting with distance is large, in the range of 1.1–1.6 Å<sup>-1</sup>. The lower value of 1.1 Å<sup>-1</sup> is similar to the value calculated for certain saturated hydrocarbon bridges.<sup>10d</sup> The orientation angle dependence of the splitting is weak. It does not matter

**TABLE 5: KT HF/3-21G  $\Delta E(\pi^*)$  Splitting Energies (eV) Obtained from the Application of Twist-Type B to 1(*n*)**

<i>n</i>	$\Delta E(\pi^*)$ (eV) for specified twist angles <sup>a</sup>					
	6°	12°	15°	18°	24°	30°
1	0.1065	0.1065	0.1068	0.1070	0.1073	0.1075
2	0.01693	0.01688	0.01684	0.01681	0.01676	0.01674
3	0.00245	0.00244	0.00243	0.00242	0.00242	0.00241
4	$3.32 \times 10^{-4}$	$3.30 \times 10^{-4}$	$3.29 \times 10^{-4}$	$3.28 \times 10^{-4}$	$3.27 \times 10^{-4}$	$3.26 \times 10^{-4}$
5	$4.30 \times 10^{-5}$	$4.28 \times 10^{-5}$	$4.27 \times 10^{-5}$	$4.25 \times 10^{-5}$	$4.23 \times 10^{-5}$	$4.23 \times 10^{-5}$
6	$5.41 \times 10^{-6}$	$5.39 \times 10^{-6}$	$5.37 \times 10^{-6}$	$5.32 \times 10^{-6}$	$5.32 \times 10^{-6}$	$5.31 \times 10^{-6}$

<sup>a</sup> The 0° twist values are identical to those obtained for twist-type A (Table 1, text), and therefore have been omitted.

**TABLE 6: KT HF/3-21G  $\Delta E(\pi^*)$  Splitting Energies (eV) Obtained from the Application of Twist-Type C to 1(*n*)**

<i>n</i>	$\Delta E(\pi^*)$ (eV) for specified twist angles <sup>a</sup>							
	6°	12°	18°	24°	30°	36°	42°	45°
1	0.1037	0.09688	0.08584	0.07106	0.05304	0.03241	0.01004	0.00147
2	0.01657	0.01546	0.01367	0.01127	0.00838	0.00511	0.00162	$1.62 \times 10^{-4}$
3	0.00240	0.00224	0.00197	0.00163	0.00121	$7.37 \times 10^{-4}$	$2.35 \times 10^{-4}$	$2.08 \times 10^{-5}$
4	$3.25 \times 10^{-4}$	$3.02 \times 10^{-4}$	$2.67 \times 10^{-4}$	$2.20 \times 10^{-4}$	$1.63 \times 10^{-4}$	$9.96 \times 10^{-5}$	$3.19 \times 10^{-5}$	$2.61 \times 10^{-6}$
5	$4.21 \times 10^{-5}$	$3.92 \times 10^{-5}$	$3.46 \times 10^{-5}$	$2.85 \times 10^{-5}$	$1.29 \times 10^{-5}$	$1.29 \times 10^{-5}$	$4.14 \times 10^{-6}$	$3.3 \times 10^{-7}$
6	$5.30 \times 10^{-6}$	$4.39 \times 10^{-6}$	$4.36 \times 10^{-6}$	$3.58 \times 10^{-6}$	$2.66 \times 10^{-6}$	$1.62 \times 10^{-6}$	$5.2 \times 10^{-7}$	$4 \times 10^{-8}$

<sup>a</sup> The 0° twist values are identical to those obtained for twist-type A (Table 1, text), and therefore have been omitted.

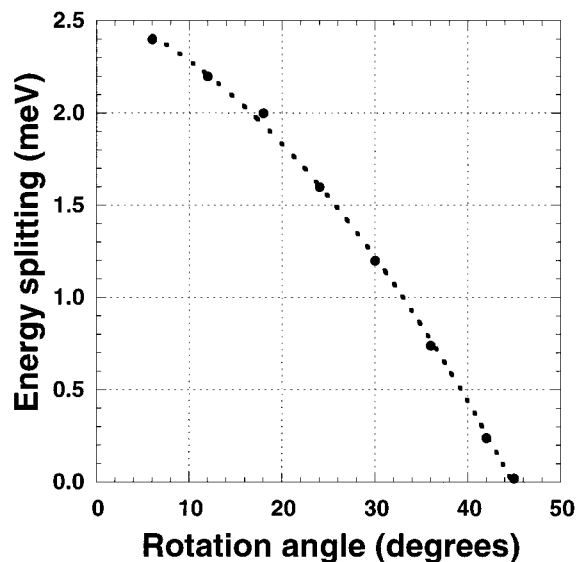


**Figure 4.** Dependence of KT HF/3-21G energy splitting for twist type C (benzene stack fixed, TCNEs rotated) for the 1(3) stack.

whether (1) the rings are rotated with fixed TNCE orientations, or (2) the TCNEs are rotated with fixed ring positions. This result is in contrast to the results seen for benzene rings interacting in an edge-on fashion.<sup>25</sup>

As expected, we found that the  $\beta_e$  values calculated using the CNDO semiempirical method are larger than those computed using the ab initio approach. The asymptotic decay of the coupling in the semiempirical method is determined by the decay exponents associated with the Slater orbitals employed. This contrasts the greater flexibility of the ab initio orbital basis which contains components with multiple decay lengths. Preliminary analysis shows that the 3-21G basis set underestimates longer range (>4 Å) through-space interactions. Indeed, basis set dependences and possible artifacts that arise in finite basis computations are of long-standing interest in electron transport theory.<sup>1,10,16,19</sup>

Ongoing experimental and computational studies are underway to explore further the dependence of electron tunneling interactions upon bridge structure, basis set, tunneling energy, donor/acceptor structure, and distortion modes of the bridge.

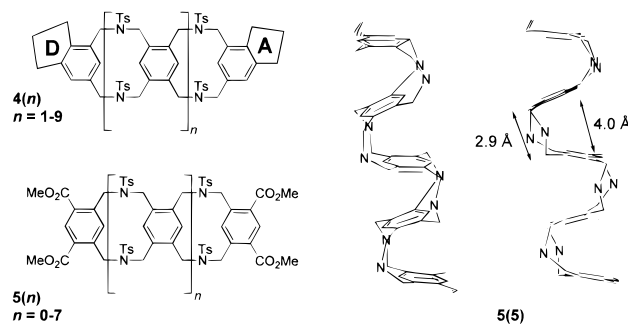


**Figure 5.** Proposed systems, 4(*n*), for the experimental determination of the distance dependence of the dynamics of electron transfer through well-defined stacks of benzene rings, based on the known ribbons 5(*n*).<sup>26</sup> Right-hand side: Part of the X-ray structure of 5(5).<sup>26a</sup> The tosyl groups have been omitted for clarity.

The series 4(*n*) (Figure 5), based on the known ribbons 5(*n*),<sup>26</sup> should be ideal for studying  $\pi$ -stack mediated electron transfer processes because X-ray crystal structures and <sup>1</sup>H NMR studies on members of 5(*n*) reveal that these molecules adopt the folded *syn* conformation in which the benzene rings lie on top of each other in approximately parallel planes, the average distance between adjacent benzene rings being 3.4 Å.<sup>26</sup> The  $\pi$ -stack interactions in the systems examined here are sensitive to the computational methodology and basis set because of the role played by nonbonded (or through-space) interactions. However, because of the nearest-neighbor dominance of through-space propagation in  $\pi$ -stacks, modest Gaussian basis sets suffice, and an ab initio divide-and-conquer approach with such modest basis sets may prove useful.<sup>16</sup>

**Acknowledgment.** We thank J. K. Barton for stimulating discussions. The research at the United States sites is supported by a grant from the National Institutes of Health (GM-57876). The research at the University of New South Wales is supported by the Australian Research Council. M.N.P.-R. additionally thanks the ARC for the award of an ARC Senior Research Fellowship. We acknowledge the New South Wales Centre for Parallel Computing for a generous allocation of computer time. D.N.B. also thanks the Burroughs-Wellcome Fund, the J. S. Guggenheim Foundation, and All Souls College, Oxford, for additional support.

**Supporting Information Available:** Tables of computed CNDO energy splittings for twist types B and C. This material is available free of charge via the Internet at <http://pubs.acs.org>.

## References and Notes

- Jortner, J.; Bixon, M. Eds., *Adv. Chem. Phys.* **1999**, *106*, *Electron transfer: From isolated molecules to biomolecules*, Parts One and Two.
- (a) Priyadarshy, S.; Risser, S. M.; Beratan, D. N. *J. Phys. Chem. A* **1996**, *100*, 17678–17682. (b) Beratan, D. N.; Priyadarshy, S.; Risser, S. M. *Chem. Biol.* **1997**, *4*, 3–8.
- Bixon, M.; Giese, B.; Wessely, S.; Langenbacher, T.; Michel-Beyerle, M. E.; Jortner, J. *Proc. Natl. Acad. Sci. U.S.A.* **1999**, *96*, 11713–11716.
- (a) Lewis, F. D.; Wu, T. F.; Zhang, Y. F.; Letsinger, R. L.; Greenfield, S. R.; Wasielewski, M. R. *Science* **1997**, *277*, 673–676. (b) Fukui, K.; Tanaka, K. *Angew. Chem., Int. Ed. Engl.* **1998**, *37*, 158–161. (c) Kelley, S. O.; Barton, J. K. *Science* **1999**, *283*, 375–381. (d) Wan, C. Z.; Fiebig, T.; Kelley, S. O.; Treadway, C. R.; Barton, J. K.; Zewail A. H. *Proc. Natl. Acad. Sci. U.S.A.* **1999**, *96*, 6014–6019. (e) Murphy, C. J.; Arkin, M. R.; Jenkins, Y.; Ghatlia, N. D.; Bossmann, S. H.; Turro, N. J.; Barton, J. K. *Science* **1993**, *262*, 1025–1029. (f) Meade, T. J.; Kayyem, J. F. *Angew. Chem., Int. Ed. Engl.* **1995**, *34*, 352–354. (g) Meade, T. J. In *Metal Ions in Biological Systems*; Sigel, H., Sigel, A., Eds.; Marcel Dekker: New York, 1995; Vol. 32, Chapter 13. (h) Giese B.; Wessely S.; Spormann M.; Lindemann U.; Meggers E.; Michel-Beyerle M. E. *Angew. Chem., Int. Ed. Engl.* **1999**, *38*, 996–998. (i) Meggers, E.; Michel-Beyerle, M. E.; Giese, B. *J. Am. Chem. Soc.* **1998**, *120*, 12950–12955. (j) Meggers E.; Kusch D.; Spichty M.; Wille U.; Giese B. *Angew. Chem., Int. Ed. Engl.* **1998**, *37*, 460–462. (k) Henderson, P. T.; Jones, D.; Hampikian G.; Kan, Y. Z.; Schuster, G. B. *Proc. Natl. Acad. Sci. U.S.A.* **1999**, *96*, 8353–8358.
- (a) Okada, A.; Chernyak, V.; Mukamel, S. *J. Phys. Chem. A* **1998**, *102*, 1241–1251. (b) Felts, A. K.; Pollard, W. T.; Friesner, R. A. *J. Phys. Chem.* **1995**, *99* (9), 2929–2940. (c) Jortner J.; Bixon M.; Langenbacher T.; Michel-Beyerle M. E. *Proc. Natl. Acad. Sci. U.S.A.* **1998**, *95*, 12759–12765. (d) Ratner, M. *Nature* **1999**, *397*, 480–481.
- Holmlin, R. E.; Tong, R. T.; Barton, J. K. *J. Am. Chem. Soc.* **1998**, *120*, 9724–9725.
- In the case of  $\mathbf{1}(n)$ ,  $n$  refers to the number of benzene rings forming the bridge.
- (a) Paddon-Row, M. N.; Wong, S. S.; Jordan, K. D. *J. Am. Chem. Soc.* **1990**, *112*, 1710–1722. (b) Jordan, K. D.; Paddon-Row, M. N. *J. Phys. Chem.* **1992**, *96*, 1188–1196. (c) Paddon-Row, M. N.; Jordan, K. D. *J. Am. Chem. Soc.* **1993**, *115*, 2952–2960. (d) Jordan, K. D.; Paddon-Row, M. N. *Electronic Coupling Through Saturated Bridges: Encyclopedia of Computational Chemistry*; Schleyer, P. v. R., Ed.; Wiley: New York, 1998; pp 826–835. (e) Shephard, M. J.; Paddon-Row, M. N. *Chem. Phys. Lett.* **1999**, *301*, 281–286.
- (a) Liang, C.; Newton, M. D. *J. Phys. Chem.* **1992**, *96*, 2855–2866. (b) Liang, C.; Newton, M. D. *J. Phys. Chem.* **1993**, *97*, 3199–3211. (d) Naleway, C. A.; Curtiss, L. A.; Miller, J. R. *J. Phys. Chem.* **1993**, *97*, 4050–4058. (c) Curtiss, L. A.; Naleway, C. A.; Miller, J. R. *Chem. Phys.* **1993**, *176*, 387–405.
- (a) Paddon-Row, M. N.; Jordan, K. D. *Modern Models of Bonding and Delocalization*; Liebman, J. F., Greenberg, A., Eds.; VCH Publishers: New York, 1988; Vol. 6, pp 115–194. (b) Jordan, K. D.; Paddon-Row, M. N. *Chem. Rev.* **1992**, *92*, 395–410. (c) Shephard, M. J.; Paddon-Row, M. N.; Jordan, K. D. *J. Am. Chem. Soc.* **1994**, *116*, 5328–5333. (d) Paddon-Row, M. N.; Shephard, M. J. *J. Am. Chem. Soc.* **1997**, *119*, 5355–5365.
- Binkley, J. S.; Pople, J. A.; Hehre, W. J. *J. Am. Chem. Soc.* **1980**, *102*, 939–947.
- The effect that other types of distortions may have on the coupling in  $\mathbf{1}(n)$ , such as the combined translational/rotational twisting that would result in a helical structure, were not examined because the computational methods used require that the two TCNE units be related by symmetry.
- The symmetries possessed by the complexes  $\mathbf{1}(n)$  after application of such twists are:  $D_{2h}$ , for the  $30^\circ$  twist of twist-types A and B;  $C_{2h}$  symmetry for the remaining twist angles of twist-type B; all remaining twist angles of twist-type A and all twist angles for twist-type C possess  $D_2$  symmetry.
- (a) Frisch, M. J.; Trucks, G. W.; Schlegel, H. B.; Gill, P. M. W.; Johnson, B. G.; Robb, M. A.; Cheeseman, J. R.; Keith, T.; Petersson, G. A.; Montgomery, J. A.; Raghavachari, K.; Al-Laham, M. A.; Zakrzewski, V. G.; Ortiz, J. V.; Foresman, J. B.; Cioslowski, J.; Stefanov, B. B.; Nanayakkara, A.; Challacombe, M.; Peng, C. Y.; Ayala, P. Y.; Chen, W.; Wong, M. W.; Andres, J. L.; Replogle, E. S.; Gomperts, R.; Martin, R. L.; Fox, D. J.; Binkley, J. S.; Defrees, D. J.; Baker, J.; Stewart, J. P.; Head-Gordon, M.; Gonzalez, C.; Pople, J. A. *Gaussian 94*; Gaussian Inc.: Pittsburgh, PA, 1995.
- Larsson, S.; Braga, M. *Int. J. Quantum Chem. Quantum Biol. Symp.* **1993**, *20*, 65–76.
- Kurnikov, I. V.; Beratan, D. N. *J. Chem. Phys.* **1996**, *105*, 9561–9573.
- Priyadarshy, S.; Skourtis, S. S.; Risser, S. M.; Beratan, D. N. *J. Chem. Phys.* **1996**, *105*, 9561–9573.
- McConnell, H. M. *J. Chem. Phys.* **1961**, *35*, 508–515.
- (a) Beratan, D. N.; J. J. Hopfield, J. J. *J. Am. Chem. Soc.* **1984**, *106*, 1584–1594. (b) Onuchic, J. N.; Beratan, D. N. *J. Am. Chem. Soc.* **1987**, *109*, 6771–6778. (c) Marvau, V.; Launay, J. P.; Joachim, C. *Chem. Phys.* **1993**, *177*, 23–30. (d) Paddon-Row, M. N. *Acc. Chem. Res.* **1994**, *27*, 18–25. (e) Jordan, K. D.; Paddon-Row, M. N. *Chem. Rev.* **1992**, *92*, 395–410. (f) Shephard, M. J.; Paddon-Row, M. N.; Jordan, K. D. *Chem. Phys.* **1993**, *176*, 289–304. (g) Cheng, J.; Sàghi-Szabó, G.; Tossell, J. A.; Miller, C. J. *J. Am. Chem. Soc.* **1996**, *118*, 680–684.
- The subscript “h” in  $\beta_h$  is used to indicate that  $\beta_h$  is derived from splitting energies,  $\Delta E(\pi)$ , involving filled  $\pi$  orbitals and hence is related to a hole transfer process.
- Falcetta, M. F.; Jordan, K. D. *J. Am. Chem. Soc.* **1991**, *113*, 2903–2909.
- Paddon-Row, M. N.; Shephard, M. J.; Jordan, K. D. *J. Am. Chem. Soc.* **1993**, *115*, 3312–3313.
- The HOMO energies of the one-benzene and two-benzene  $\pi$ -stacks are, respectively,  $-9.22$  and  $-8.38$  eV, and the LUMO energies are 4.12 and 3.79 eV, respectively.
- (a) Heilbronner, E.; Schmelzer, A. *Helv. Chim. Acta* **1975**, *58*, 936–967. (b) Paddon-Row, M. N. *Acc. Chem. Res.* **1982**, *15*, 245–251. (c) Hoffmann, R.; Imamura, A.; Hehre, W. J. *J. Am. Chem. Soc.* **1968**, *90*, 1499–1509. (d) Paddon-Row, M. N. *J. Chem. Soc., Perkin Trans. 2* **1985**, 257–263.
- (a) Helms, A.; Heiler, D.; McLendon, G. *J. Am. Chem. Soc.* **1991**, *113*, 4325–4327. (b) Helms, A.; Heiler, D.; McLendon, G. *J. Am. Chem. Soc.* **1992**, *114*, 6227–6238.
- (a) Breidenbach, S.; Ohren, S.; Nieger, M.; Vögtle, F. *J. Chem. Soc., Chem. Commun.* **1995**, 1237–1238. (b) Breidenbach, S.; Ohren, S.; Vögtle, F. *Chem. Eur. J.* **1996**, *2*, 832–837. (c) Breidenbach, S.; Ohren, S.; Herbstirmer, R.; Kotila, S.; Nieger, M.; Vögtle, F. *Liebigs Ann. Chem.* **1996**, 2115–2121. (d) Boomgaarden, W.; Vögtle, F.; Nieger, M.; Hupfer, H. *Chem. Eur. J.* **1999**, *5*, 345–355. (e) Therien, M. J. Private communication, 1999.